Coherence parameter measurements for electrons scattering off heavy noble gas targets

J. Phys. B: At. Mol. Opt. Phys. 24 (1991) 1069-1085. Printed in the UK

Coherence parameter measurements for electrons scattering off heavy noble gas targets

J J Corr, P J M van der Burgt, P Plessis†, M A Khakoo‡, P Hammond§ and J W McConkey

Department of Physics, University of Windsor, 401 Sunset Avenue, Windsor, Ontario N9B 3P4 Canada

Received 11 May 1990, in final form 7 November 1990

Abstact. Electron impact excitation of the resonance levels of Ne, Ar, Kr and Xe has been studied for electron scattering angles up to 50° and impact energies between 30 and 80 eV. The P_1 and P_4 Stokes parameters have been measured in each case so that the influence of spin in the excitation process could be studied through evaluation of ρ_{00}, the relative spin-flip cross section. After careful account was taken of various depolarizing effects due particularly to the finite volume of the interaction region and, in the cases of Kr and Xe, to nuclear spin, very good agreement has been found with theoretical predictions thus resolving a previously reported discrepancy. No evidence has been found for spin-flip under the experimental parameters used in this study, even for the heaviest target studied.

1. Introduction

The study of electron impact excitation of atoms using the electron-photon coincidence technique has elucidated many of the processes involved in these interactions and this work has been extensively reviewed and discussed (Blum and Kleinpoppen 1979, McConkey 1979, Hanne 1983, Slevin 1984, Andersen *et al* 1986, 1988, Slevin and Chwirot 1990). For the widely studied 2^1P excitation of He, *LS* coupling holds strictly and the spin of the continuum electron can be factored out of the problem. Thus the positive reflection symmetry, with respect to the scattering plane, of the atomic wavefunction is conserved during the collision. For the heavier noble gases *LS* coupling is no longer strictly valid and electron spin may play a role in the excitation. Consequently states having negative reflection symmetry with respect to the scattering plane may also be excited. In classical terms the excitation of an oscillator perpendicular to the scattering plane is now possible.

In previous communications from this laboratory (Khakoo and McConkey 1986, 1987) data for the out-of-plane linear and circular Stokes parameters for Ne, Ar and Kr were presented. These enabled a study of that part of the problem to which positive reflection symmetry applies and, most significantly, the circular polarization measurements enabled the sign of the angular momentum transfer in the collisions to be unambiguously determined for the electron scattering angles and incident energies considered. For incident electron energies in the range 60–80 eV and small scattering angles (<30°) angular momentum transfer is positive and surprisingly similar for all the targets considered (see also McConkey *et al* 1988). Measured total polarizations of close to unity suggested that essentially full coherence of this part of the excitation was occurring.

† Permanent address: Department of Physics, Laurentian University, Sudbury, Ontario, Canada.
‡ Permanent address: Department of Physics, California State University, Fullerton, CA, USA.
§ Permanent address: Department of Physics, University of Manchester, UK.

0953-4075/91/051069+17$03.50

More recently Plessis *et al* (1988) reported the first in-plane polarization correlation Stokes parameter measurements for Kr and Xe. They noted large deviations of their measured P_4 parameters from unity over a certain range of electron scattering angles indicating that the excited-state charge clouds possessed significant 'height' perpendicular to the scattering plane. They suggested that their measurements of a non-zero ρ_{00} (height) parameter were due to a breakdown of the reflection symmetry (with respect to the scattering plane) in the excitation process caused by a spin flip of the exciting electron.

Since such a process is unexpected on theoretical grounds for the small scattering angles considered in these experiments, there has been considerable activity in our laboratory and others to see if this and similar data could be accounted for by experimental effects, particularly those related to the fact that the interaction region has a finite volume. This causes some loss of definition of the scattering plane to occur particularly at small scattering angles. A number of authors (Martus *et al* 1988, Martus and Becker 1989, Hanne 1990, McConkey *et al* 1990, Zetner *et al* 1989, 1990) have demonstrated that indeed, under certain experimental conditions, considerable deviations of measured Stokes parmeters from actual ones can be expected both for polarization correlation measurements of the type discussed in this work and also for the time-inverse type of measurements where electrons are scattered superelastically from laser-excited targets. Very recently Simon *et al* (1990) have carefully investigated such effects in their study of electron impact excitation of $Hg(^3P_1)$ and in a companion paper (van der Burgt *et al* 1991) we discuss our analysis of these problems as they relate to our measurements in the heavy rare gases.

Previous experimental measurements relevant to the present work have considered the excitation of Kr and Xe targets (McGregor *et al* 1982, Danjo *et al* 1985, King *et al* 1985, Nishimura *et al* 1986, Murray *et al* 1990). In all cases the data have been obtained using angular correlation techniques. Theoretical calculations of Stokes or equivalent parameters have been carried out for Ne (Machado *et al* 1982), Ar (da Paixao *et al* 1984) and Kr (Meneses *et al* 1985) using first-order many-body theory (FOMBT). Recently Bartschat and Madison (1987), using a distorted-wave Born approximation (DWBA), have investigated the importance of relativistic spin-dependent effects both on the description of the Ne, Ar, Kr, Xe target states and on the wavefunction of the continuum electron. For the small scattering angles involved in this work these effects were found to be small even for a heavy target such as Xe.

In all the earlier work on the heavy rare gases there was no consideration of hyperfine depolarizing interactions. In this paper we show that these play a crucial role for Kr and Xe and by comparison, experimental effects of the type mentioned above are small. Proper consideration of all of these effects resolve the previous discrepancies between experimental measurements and theoretical predictions. In section 2 we present some basic theory, in section 3 we provide the salient experimental details and in section 4 we present and discuss our results for Ne, Ar, Kr and Xe. Our findings are summarized in section 5.

2. Basic theory

The density matrix description of the excitation of the heavier noble gases leads to a formulation involving five independent parameters rather than only three for the simpler case of He. These parameters and their relation to experimentally measurable angular

correlation or polarization correlation parameters have been outlined in the reviews mentioned above. We refer in particular to Anderson *et al* (1988) who provide a complete listing of formulae linking the various parameters used by different authors. The initial set of these parameters were the σ, λ, $\bar{\chi}$, $\cos\varepsilon$ and $\cos\Delta$ parameters introduced by Blum *et al* (1980) and da Paixao *et al* (1980). More recently Andersen *et al* (1986, 1988) have introduced the σ, $L_\perp^+$, γ, P_1^+ and ρ_{00} parameters which give a more transparent description of the excitation process in terms of the excited-state charge cloud characteristics. These latter parameters relate in a particularly simple way to our polarization correlation measurements (Khakoo and McConkey 1987).

Since we are interested in charge cloud height determinations we concentrate on the P_1 and P_4 linear polarization parameters and the ρ_{00} parameter. The ρ_{00} parameter gives the relative probability for spin flip perpendicular to the scattering plane and, in terms of charge cloud characteristics, it gives the relative height of the charge cloud. Alternatively since the excited P state radiates like a set of mutually orthogonal classical oscillators we may consider ρ_{00} as giving the relative strength of the oscillator perpendicular to the scattering plane (Andersen *et al* 1988). ρ_{00} is related to the measurable Stokes parameters by the following equation (Anderson *et al* 1986, 1988):

$$\rho_{00}=\frac{(1+P_1)(1-P_4)}{4-(1-P_1)(1-P_4)} \tag{1}$$

where P_1 and P_4 monitor the number of coincidences with photons polarized parallel to the incident electron beam minus those polarized perpendicular to this beam normalized to the total number of coincidence events, as detected by photon polarization analysers placed above the scattering plane (P_1) and in the scattering plane (P_4) respectively. In a polarization correlation experiment both in-plane and out-of-plane polarization measurements are required. Similarly if angular correlation experiments are carried out, the radiation pattern must be probed in three dimensions and at least two out-of-the-scattering-plane measurements are needed.

Clearly before any evaluation of ρ_{00} is made the measured Stokes parameters must be corrected for any experimental or other depolarizing effects. Van der Burgt *et al* (1991) have given an extensive discussion of the effects due to a finite interaction volume and due to hyperfine interaction. In this section we discuss how the measured Stokes parameters P_1^{M} and P_4^{M} can be corrected for finite interaction volume effects to obtain the time-averaged Stokes parameters P_1' and P_4'. These parameters can be corrected for hyperfine interaction so that the parameters P_1 and ρ_{00} are obtained, which relate to the nascent charge cloud.

The model used here to correct for finite interaction volume effects is the approximate analytical model of van der Burgt *et al* (1991). We use their equations (3.26) and (3.27), which relate the measured Stokes parameters to the time-averaged Stokes parameters:

$$P_1^{\mathrm{M}}=\frac{1-\left(\dfrac{1-P_1'}{1+P_1'}\right)(1-\mu)-\left(\dfrac{1-P_4'}{1+P_4'}\right)\mu}{1+\left(\dfrac{1-P_1'}{1+P_1'}\right)(1-\mu)+\left(\dfrac{1-P_4'}{1+P_4'}\right)\mu} \tag{2}$$

$$P_4^{\mathrm{M}} = \frac{1 - \left(\frac{1-P_1'}{1+P_1'}\right)\mu - \left(\frac{1-P_4'}{1+P_4'}\right)(1-\mu)}{1 + \left(\frac{1-P_1'}{1+P_1'}\right)\mu + \left(\frac{1-P_4'}{1+P_4'}\right)(1-\mu)} \tag{3}$$

where $\mu = \overline{\sin^2\beta} = r^2/4R_e^2 \sin^2\theta_e$ and β defines the angle of rotation of the effective scattering plane due to finite volume or other effects (see figure 1 of van der Burgt *et al* 1991). We note that even if $P_4' = 1$ a significant effect can arise for small electron scattering angles where large variations in β can occur. Further this is amplified if $P_1' < 1$, a situation which arises for small angle scattering in the heavy rare gases.

In the approximate analytical model used here it is readily possible to invert equations (2) and (3) to obtain the time-averaged Stokes parameters P_i' from the measured ones, P_i^{M}. Thus

$$P_1' = \frac{1 - \left(\frac{1-P_1^{\mathrm{M}}}{1+P_1^{\mathrm{M}}}\right)\left(\frac{1-\mu}{1-2\mu}\right) - \left(\frac{1-P_4^{\mathrm{M}}}{1+P_4^{\mathrm{M}}}\right)\left(\frac{-\mu}{1-2\mu}\right)}{1 + \left(\frac{1-P_1^{\mathrm{M}}}{1+P_1^{\mathrm{M}}}\right)\left(\frac{1-\mu}{1-2\mu}\right) + \left(\frac{1-P_4^{\mathrm{M}}}{1+P_4^{\mathrm{M}}}\right)\left(\frac{-\mu}{1-2\mu}\right)} \tag{4}$$

$$P_4' = \frac{1 - \left(\frac{1-P_1^{\mathrm{M}}}{1+P_1^{\mathrm{M}}}\right)\left(\frac{-\mu}{1-2\mu}\right) - \left(\frac{1-P_4^{\mathrm{M}}}{1+P_4^{\mathrm{M}}}\right)\left(\frac{1-\mu}{1-2\mu}\right)}{1 + \left(\frac{1-P_1^{\mathrm{M}}}{1+P_1^{\mathrm{M}}}\right)\left(\frac{-\mu}{1-2\mu}\right) + \left(\frac{1-P_4^{\mathrm{M}}}{1+P_4^{\mathrm{M}}}\right)\left(\frac{1-\mu}{1-2\mu}\right)}. \tag{5}$$

In practice we find that for our experimental arrangement to a very good approximation, $P_i' = P_i^{\mathrm{M}}$ for $i = 1, 2$, and 3 and so we only correct P_4^{M} to get P_4' in this way.

Even after suitable allowance for experimental effects have been made it is important to take account of any other depolarizing effects which may be occurring. If a significant fraction of the target atoms have non-zero nuclear spin and if the lifetimes of the excited states are long compared to the hyperfine interaction time then a depolarization will occur, and correction factors must be introduced to obtain the Stokes parameters, P_i, which describe the nascent (collision-induced) charge cloud from the time averaged parameters P_i'. These are (Andersen *et al* 1988):

$$P_i = P_i'\left[\frac{2 + G_2(1 - 3\rho_{00})}{3G_2(1-\rho_{00})}\right] \qquad i = 1, 2 \tag{6}$$

$$P_3 = P_3'\left[\frac{2 + G_2(1 - 3\rho_{00})}{3G_1(1-\rho_{00})}\right] \tag{7}$$

ρ_{00} is obtained from

$$\rho_{00} = \frac{1}{3} - \frac{2}{3G_2}\left[\frac{2P_4' - P_1' + P_1'P_4'}{4 - (1-P_1')(1-P_4')}\right] \tag{8}$$

and G_1, G_2 are the appropriate depolarization factors for the P-S transition involved (Andersen *et al* 1988, Blum 1981).

Details of these factors and other information relative to the reduction of the data are given in section 3.

3. Experiment

The experimental set-up has been described in earlier papers (Becker *et al* 1984, Khakoo and McConkey 1986, 1987), therefore only the pertinent details will be given here. A schematic diagram of the apparatus is given in figure 1 of the paper by Plessis *et al* (1988). For some measurements, the gas inlet system indicated by Plessis *et al* (1988) was replaced by one where the gas and electron beams were orthogonal to each other and to the optic axis of the P_4 detector. This provided a more symmetrical arrangement for investigation of finite volume effects. In practice essentially identical results were obtained using both systems. The radius, r, of the electron beam in the interaction region was estimated from the calculated and measured performance parameters of the gun, from the 'burn' mark in the Faraday cup, and from the fact that no measurable current due to the electron beam was detected on the gas needles. It did not exceed 1 mm for the measurements reported here. The distance R_e from the interaction region to the entrance aperture of the analyser was 28.5 mm.

Standard techniques are used to measure the polarization of the photons emitted perpendicular to the scattering plane (linear and circular polarization) as well as in the scattering plane. The in-plane linear polarization analyser consists of a single, gold-coated mirror with an angle of incidence of 57.5°. It is situated at right angles to the incident electron beam direction. Both photons and inelastically scattered electrons are detected by channel electron multipliers (CEM). Coating the entrance cones of the photon CEM with cesium iodide significantly enhanced their detection efficiency above 100 nm (Johnson 1969), where the resonance transitions of Ar, Kr and Xe lie.

Research purity (99.995) neon, argon, krypton and xenon were used as the target gases and were introduced into the interaction region through a single capillary. A pressure increase of 1.5×10^{-7} Torr or less above background was maintained during data collection in order to render negligible any radiation trapping effects. An electron gun produced the electron beam and scattered electrons were energy selected by a hemispherical analyser. Electron beam currents of several μA were easily obtained with an energy resolution of approximately 600 meV (FWHM). This resolution was insufficient to resolve the $[\frac{1}{2}]_1^0\, ns'\,{}^1P$ and $[\frac{3}{2}]_1^0\, ns\,{}^3P$ peaks (Racah notation) in Ne and Ar. The Kr peaks were only partially resolved. For the electron scattering angular range studied here the ^1P peaks of Ne and Ar were approximately five times the intensity of the respective ^3P peaks and so for these targets the data are predominantly due to singlet excitation even though the transitions were not resolved. In Kr the contribution from the adjacent peak was less than 10% while in Xe the two peaks were completely resolved.

The polarization efficiency of the linear polarizers can be calculated using the known optical constants of gold. However the efficiency also depends on the surface cleanliness of the gold mirrors which was found to vary slowly with time though this effect was greatly reduced when an oil free backing pump was coupled with the turbo molecular pump evacuating the system. The P_4 mirror could be heated to about 70 °C to reduce vapour condensation on its surface. The polarization efficiency drops as the mirror contamination increases. To account for this effect and also to check the spectral alignment of the system, non-coincidence polarization measurements with the P_1 or P_4 analyser were taken before and after each coincidence measurement. The average of these measurements was then compared to the largest non-coincidence value obtained during the course of this study and the ratio between these values was then used to scale up the measured values. These scaling-up factors varied between 1.004

and 1.226 for the P_4 measurements over the entire time period of the investigation. The possible error in an individual measurement due to this effect is less than 5%. This correction was not necessary for the P_1 measurements since a double mirror linear polarizer is employed in this case whose resulting polarization efficiency is considerably less affected by small variations in the quality of the mirror surfaces (see Hammond *et al* 1989).

3.1. Data reduction

As indicated in section 2, various corrections need to be applied to the raw data to take account of finite volume effects and the finite angular acceptance of the detectors. These have been discussed in detail by van der Burgt *et al* (1991) who illustrate the magnitude of the effects due to finite electron beam size and displacement, lack of parallelism of the electron beam etc. They show that those effects are small under realistic experimental conditions. Further, very similar results were obtained either if the data reduction was carried out using a simple analytical model or by carrying out a full numerical analysis. The non-coincidence polarization measurements mentioned in the previous section provided a good indication (from the symmetry of the observed radiation pattern) that the system was accurately aligned, and hence that finite volume effects were minimized.

To properly allow for hyperfine depolarization effects we assume the natually occurring percentages of odd isotopes given by Heath (1984). These percentages and the appropriate nuclear spins are included in table 1. Only in Kr and Xe do we expect any effect. Because the natural widths of these levels are only a few hundreds of MHz (lifetimes of a few *n*s for both Kr and Xe (Matthias *et al* 1977)) whereas the hyperfine splitting is hundreds or thousands of MHz (Lederer and Shirley 1978, Husson *et al*

Table 1. Isotope data for the heavy rare gases.

Isotope[a]	Abundance (%)	Nuclear Spin	Depolarizing factor G_1	Depolarizing factor G_2	Net G factors[b] G_1	Net G factors[b] G_2
Kr^{78}	0.35	0	1	1		
Kr^{80}	2.25	0	1	1		
Kr^{82}	11.6	0	1	1		
Kr^{83}	11.5	$\frac{9}{2}$	0.347	0.208	0.925	0.909
Kr^{84}	57.0	0	1	1		
Kr^{86}	17.3	0	1	1		
Xe^{124}	0.1	0	1	1		
Xe^{126}	0.1	0	1	1		
Xe^{128}	1.9	0	1	1		
Xe^{129}	26.4	$\frac{1}{2}$	0.778	0.333		
Xe^{130}	4.1	0	1	1	0.819	0.664
Xe^{131}	21.2	$\frac{3}{2}$	0.422	0.247		
Xe^{132}	26.9	0	1	1		
Xe^{134}	10.4	0	1	1		
Xe^{136}	8.9	0	1	1		

[a] Ne has only a 0.257% odd isotope component. Since the effect of this will be negligible the data is not listed. Naturally occurring Ar isotopes all have zero nuclear spin.

[b] These are weighted averages of the individual G factors.

1979, Jackson 1977, Jackson and Coulombe 1972) there is more than adequate time for the hyperfine interaction to occur before emission of a photon takes place. Thus in both these targets a significant depolarization is expected.

The appropriate G-values for the different nuclear spins are readily evaluated (van der Burgt *et al* 1991, Andersen *et al* 1988, Blum 1981, Nienhuis 1980) and are listed in table 1. Also listed are the net G-factors for the two gases. These take account of the relative percentages of the different isotropes in the target assuming that the signals from the different isotopes add incoherently (see Wolcke *et al* 1983).

3.2. Errors

The errors given in this work are statistical in nature and correspond to one standard deviation. The errors associated with the correction factors (discussed above) are small and difficult to estimate accurately. Consequently they have not been incorporated into the cited errors. The uncertainty in θ_e is estimated to be $\pm 1.5°$. The quoted energies are accurate to ± 1 eV.

4. Results and discussion

The data for the four target gases studied in this work are listed in tables 2–8 and displayed in figures 1–7. We note that in all cases the displayed data are measured

Table 2. Parameters for Ne at 80 eV incident energy.

θ_e (deg)	μ[b] (equations (2) and (3))	P_1^M	P_4^M	P_4' (equation (5))
5	0.041		0.99 ± 0.01	—
7.5	0.018	-0.04 ± 0.03[a]	0.97 ± 0.04	1.01 ± 0.04
10	0.010	-0.30 ± 0.02[a]	1.02 ± 0.03	1.06 ± 0.03
12.5	0.007		0.98 ± 0.06	—
15	0.005	-0.70 ± 0.02	0.84 ± 0.05	0.88 ± 0.05
17.5	0.003	-0.69 ± 0.03[a]	0.80 ± 0.08	0.83 ± 0.09
20	0.003	-0.77 ± 0.03[a]	0.83 ± 0.09	0.87 ± 0.09
30	0.001		0.97 ± 0.08	—
35	0.001	-0.08 ± 0.05[a]	0.99 ± 0.06	0.99 ± 0.06
45	0.001	0.42 ± 0.07[a]	1.10 ± 0.09	1.10 ± 0.09

[a] From Khakoo and McConkey (1987).
[b] Calculated using $r = 1$ mm and $R_e = 28.5$ mm (see text).

Table 3. Parameters for Ar at 80 eV incident energy.

θ_e (deg)	P_1^M	P_4^M	P_4' (equation (5))
5	-0.33 ± 0.02	1.00 ± 0.02	1.19 ± 0.03
10	-0.53 ± 0.05[a]	0.91 ± 0.07	0.97 ± 0.07
15	-0.76 ± 0.04[a]	0.94 ± 0.11	1.01 ± 0.02
20	-0.25 ± 0.06	1.02 ± 0.07	1.03 ± 0.07
30	0.36 ± 0.07[a]	1.04 ± 0.08	1.04 ± 0.08

[a] From Khakoo and McConkey (1987).

Table 4. Parameters for Kr $[\frac{1}{2}]_1^0$ 5s $^1P_1$ excitation at 60 eV incident energy.

θ_e (deg)	P_1^M	P_4^M	ρ_{00} (equation (8))	P_1 (equation (6))	P_4' (equation (5))
3	—	0.81 ± 0.05	—	—	—
5	−0.12 ± 0.04	0.78 ± 0.04	−0.001 ± 0.012	−0.13 ± 0.04	0.87 ± 0.05
7.5	—	0.70 ± 0.06	—	—	—
10	−0.77 ± 0.06[a]	0.63 ± 0.04	−0.015 ± 0.009	−0.82 ± 0.06	0.74 ± 0.06
12.5	—	0.56 ± 0.08	—	—	—
15	−0.50 ± 0.05[a]	0.63 ± 0.06	0.023 ± 0.013	0.53 ± 0.05	0.65 ± 0.06
17.5	—	0.78 ± 0.07	—	—	—
20	−0.04 ± 0.06[a]	0.98 ± 0.08	−0.030 ± 0.020	−0.04 ± 0.06	0.99 ± 0.08
30	0.73 ± 0.09	0.96 ± 0.05	−0.014 ± 0.026	0.78 ± 0.010	0.96 ± 0.05

[a] From Khakoo and McConkey (1987).

Table 5. Parameters for Kr $[\frac{3}{2}]_1^0$ 5s $^3P_1$ excitation at 60 eV incident energy.

θ_e (deg)	P_1^M	P_4^M	ρ_{00} (equation (8))	P_1 (equation (6))	P_4' (equation (5))
5	0.04 ± 0.04	0.83 ± 0.04	−0.001 ± 0.012	0.05 ± 0.04	0.89 ± 0.04
7.5	—	0.53 ± 0.04	—	—	—
10	−0.71 ± 0.03	0.59 ± 0.06	−0.002 ± 0.008	−0.75 ± 0.03	0.66 ± 0.07
12.5	—	0.51 ± 0.07	—	—	—
15	−0.60 ± 0.09[a]	0.66 ± 0.06	0.006 ± 0.013	−0.64 ± 0.10	0.69 ± 0.06
20	−0.14 ± 0.07[a]	0.90 ± 0.06	−0.010 ± 0.015	−0.15 ± 0.08	0.90 ± 0.06
30	0.70 ± 0.10	1.02 ± 0.09	−0.045 ± 0.041	0.75 ± 0.11	1.02 ± 0.09

[a] From Khakoo and McConkey (1987).

Table 6. Parameters for Xe $[\frac{3}{2}]_1^0$ 6s $^3P_1$ excitation at 30 eV incident energy.

θ_e (deg)	P_1^M	P_4^M	ρ_{00} (equation (8))	P_1 (equation (6))	P_4' (equation (5))
3	0.42 ± 0.06	0.75 ± 0.09	−0.064 ± 0.065	0.55 ± 0.09	0.81 ± 0.11
5	0.20 ± 0.05	0.68 ± 0.04	−0.030 ± 0.021	0.27 ± 0.07	0.71 ± 0.04
10	−0.39 ± 0.04	0.44 ± 0.03	−0.013 ± 0.014	−0.51 ± 0.05	0.46 ± 0.03
15	−0.59 ± 0.04	0.16 ± 0.04	0.023 ± 0.021	−0.79 ± 0.05	0.17 ± 0.04
20	−0.45 ± 0.03	0.21 ± 0.05	0.060 ± 0.025	−0.61 ± 0.04	0.21 ± 0.05
25	0.06 ± 0.08	0.64 ± 0.07	−0.012 ± 0.033	0.08 ± 0.11	0.64 ± 0.07
30	0.48 ± 0.08	0.89 ± 0.10	−0.107 ± 0.056	0.63 ± 0.10	0.89 ± 0.10
40	0.55 ± 0.09	0.80 ± 0.05	−0.049 ± 0.033	0.73 ± 0.12	0.80 ± 0.05
50	0.00 ± 0.08	0.57 ± 0.10	0.011 ± 0.049	0.00 ± 0.10	0.57 ± 0.10

data. In addition to the measured Stokes parameters P_1^M and P_4^M, the tables list the time-averaged Stokes parameter P_4', and (for Kr, Xe) the parameters P_1 and ρ_{00} of the nascent charge cloud, obtained by applying the corrections of section 2. For comparison purposes, other available experimental and theoretical data are included in the figures. In the case of Ne, Ar, and Kr we were able to use the P_1^+ values reported by Khakoo and McConkey (1987). A complete analysis of the P_1^+ as well as P_2^+ and P_3^+ results

Table 7. Parameters for Xe $[\frac{3}{2}]_1^0$ 6s $^3P_1$ excitation at 50 eV incident energy.

θ_e (deg)	P_1^M	P_4^M	ρ_{00} (equation (8))	P_1 (equation (6))	P_4' (equation (5))
3	—	0.73 ± 0.06	—	—	—
5	0.11 ± 0.08	0.63 ± 0.04	−0.016 ± 0.024	0.15 ± 0.10	0.66 ± 0.04
10	−0.43 ± 0.03	0.38 ± 0.04	−0.004 ± 0.017	−0.57 ± 0.04	0.40 ± 0.04
15	−0.53 ± 0.05	0.26 ± 0.04	0.010 ± 0.022	−0.71 ± 0.07	0.27 ± 0.04
20	−0.04 ± 0.09	0.52 ± 0.08	0.029 ± 0.039	−0.06 ± 0.12	0.52 ± 0.08
30	0.12 ± 0.13	0.81 ± 0.12	−0.083 ± 0.055	0.16 ± 0.17	0.81 ± 0.12
40	—	0.83 ± 0.26	—	—	—

Table 8. Parameters for Xe $[\frac{3}{2}]_1^0$ 6s $^3P_1$ excitation at 80 eV incident energy.

θ_e (deg)	P_1^M	P_4^M	ρ_{00} (equation (8))	P_1 (equation (6))	P_4' (equation (5))
5	−0.31 ± 0.04	0.37 ± 0.06	0.012 ± 0.028	−0.41 ± 0.05	0.43 ± 0.06
10	−0.58 ± 0.06	0.16 ± 0.05	0.023 ± 0.032	−0.78 ± 0.08	0.18 ± 0.05
15	−0.19 ± 0.14	0.53 ± 0.13	−0.005 ± 0.059	−0.25 ± 0.19	0.54 ± 0.13
20	0.29 ± 0.25	0.84 ± 0.23	−0.091 ± 0.119	0.38 ± 0.33	0.84 ± 0.23
25	—	0.93 ± 0.33	—	—	—

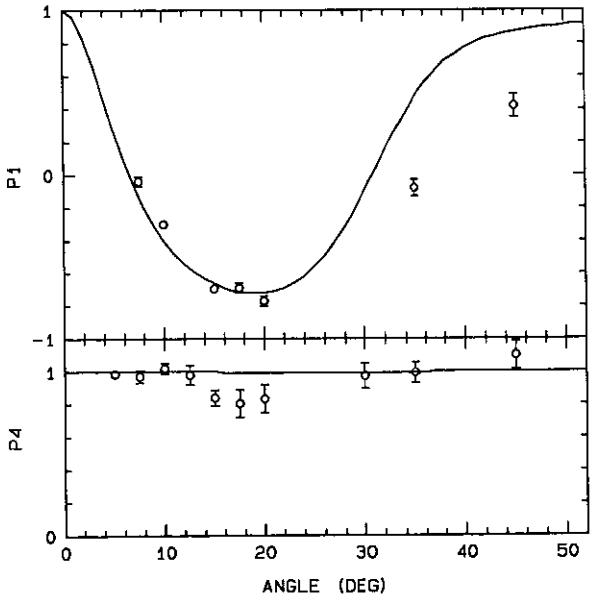

Figure 1. P_1^M and P_4^M parameters as a function of electron scattering angle for electron impact excitation of Ne at 80 eV. Open circles, present data; full curve, Bartschat and Madison (1987) DWBA. For a comparison with other experimental and theoretical P_1 data see Khakoo and McConkey (1987).

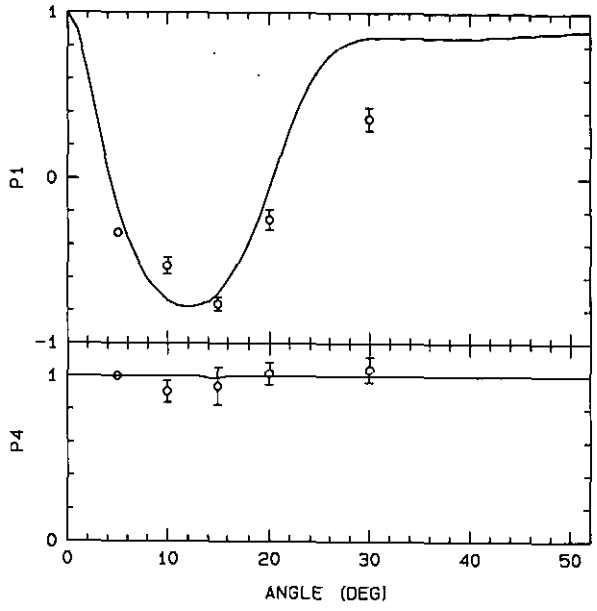

Figure 2. P_1^M and P_4^M parameters for Ar at 80 eV. Symbols as in figure 1.

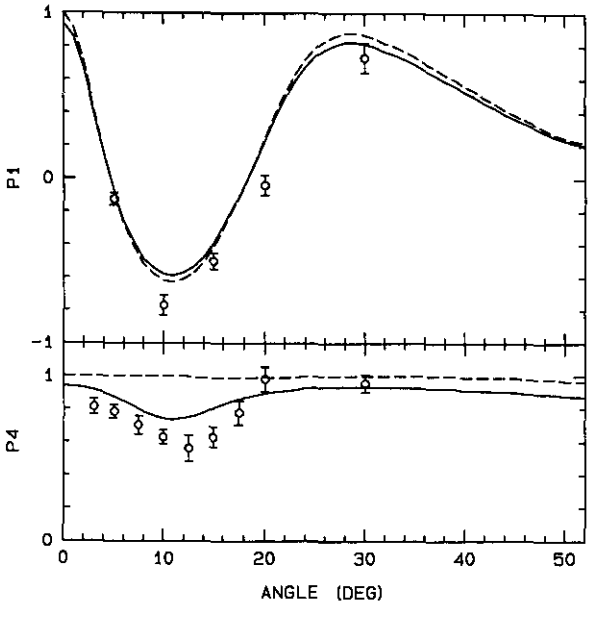

Figure 3. P_1^M and P_4^M parameters for the $[\frac{1}{2}]_1^0$ 5s′ state of Kr at 60 eV. Symbols as in figure 1 except that Bartschat and Madison's data (full curve) have also been corrected for hyperfine interaction effects. The broken curve shows the DWBA results before correction for hyperfine interaction effects.

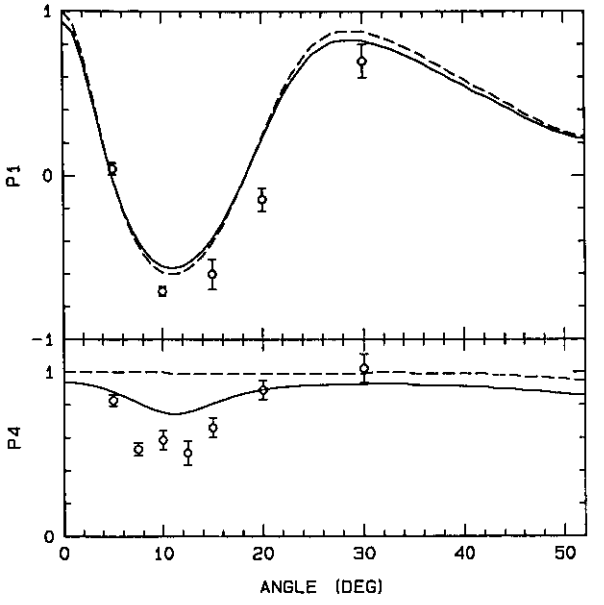

Figure 4. P_1^M and P_4^M parameters for the $[\frac{3}{2}]_1^0$ 5s state of Kr at 60 eV. Symbols as in figure 3.

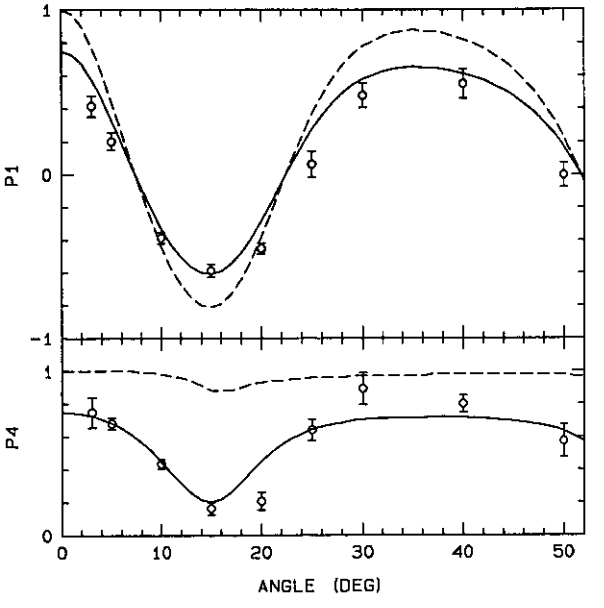

Figure 5. P_1^M and P_4^M parameters for the $[\frac{3}{2}]_1^0$ 6s state of Xe at 30 eV. Symbols as in figure 3.

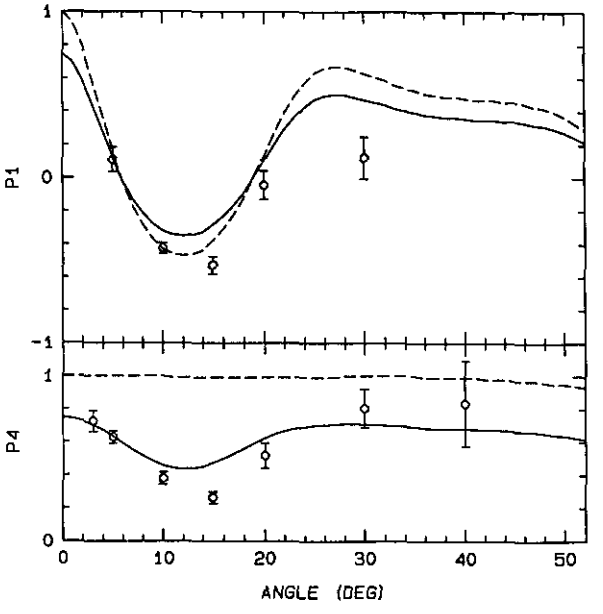

Figure 6. P_1^M and P_4^M parameters for the $[\frac{3}{2}]_1^0$ 6s state of Xe at 50 eV. Symbols as in figure 3.

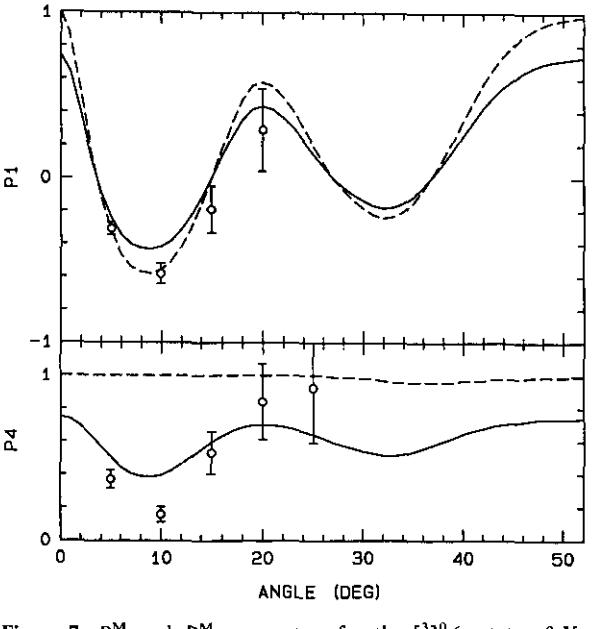

Figure 7. P_1^M and P_4^M parameters for the $[\frac{3}{2}]_1^0$ 6s state of Xe at 80 eV. Symbols as in figure 3.

for these three gases was given by these authors and so we refer the reader to this paper for a full comparison of our P_1 data with earlier work.

We note that a proper comparison can be made between our experimental data, corrected for the effect of a finite interaction region (P_1' and P_4'), and Bartschat and Madison's (1987) theoretical data (full curve in the figures). In case of Kr and Xe the theoretical data is corrected for hyperfine depolarization. As discussed in section 2 $P_1' = P_1^M$ to a very good approximation. Our P_4' data, obtained from equation (5) for those angles where P_1^M and P_4^M data are available, are included in the tables only to avoid cluttering of the figures. In most cases the difference between P_4' and P_4^M is smaller than the experimental error bar.

The P_1^M values for all target gases were in good agreement with other experimental data though very limited data was available for Ne and Ar. The best agreement with theory was with Bartschat and Madison's (1987) DWBA calculations and so, for the sake of clarity, only these are shown on the figures. It can be seen that the agreement is quite good at the smaller scattering angles up to 20°. At larger scattering angles discrepancies are more apparent. We note that Murray *et al* (1990) in their recent study of 30 eV Kr excitation, also found that the DWBA calculations were preferred.

In Kr the agreement between the measured P_1^M values and theory is satisfactory for both $[\frac{1}{2}]_1^0 5s'$ and $[\frac{3}{2}]_1^0 5s$ states though there is some indication, particularly in the latter case, that the dip in the 10°–15° region should be somewhat deeper and broader than indicated by the DWBA or other theoretical results. Inclusion of the hyperfine depolarization makes a marginal improvement in the quality of the agreement.

As far as the P_1^M parameter is concerned, the most significant comparisons with theory occur with Xe as the target gas. The largest angular range considered was at 30 eV impact energy, figure 5. In figure 5 the experimental data are compared with two theoretical curves one excluding and one including the hyperfine depolarizing effect. This figure is a clear demonstration of the significance of this effect for this target. As shown by van der Burgt *et al* (1991) finite volume and other effects can contribute at small scattering angles but have a negligible effect for $\theta_e > 20°$. At the higher incident energies in Xe, figures 6 and 7, it appears that the DWBA results again underestimate both the magnitude and width of the first dip in the P_1 data so that the inclusion of hyperfine depolarization actually worsens the level of agreement between theory and experiment in this angular region. This has implications for the P_4 data as well (equation (3)) as discussed later.

The P_4^M results for Ne and Ar (figures 1 and 2, tables 2 and 3) are essentially unity over the scattering range studied here in accord with the theoretical calculations. There is the suggestion of a slight drop in the Ne P_4^M values in the angular range where P_1^M goes through a deep minimum and a hint of a similar effect in the Ar data though these deviations from unity are barely statistically significant especially if an error of two standard deviations was considered. We note from equation (3), section 2, that if a finite volume effect was occurring it could be amplified for large negative values of P_1. We suggest that these data can be used to put an upper limit on the magnitude of these instrumental effects (see van der Burgt *et al* 1991).

The Kr P_4^M data are shown in the lower panels of figures 3 and 4 and in tables 4 and 5. Comparison is again with the theoretical data of Bartschat and Madison (1987). It is clear that the calculated curves using the theoretical data and assuming complete hyperfine depolarization largely account for the trend in the observations. If, as suggested earlier, the theoretical data underestimate the magnitude and width of the negative excursion of P_1 around $\theta_e = 10°$, then considerably improved agreement

between experiment and theory would be obtained. The $[\frac{3}{2}]_1^0 5s\ ^3P$ data demonstate somewhat more scatter perhaps indicating the presence of some finite interaction volume effects in this case.

At 30 eV in Xe (figure 5 and table 6), the agreement between experiment and predictions is good over the whole angular range providing strong support for the previous conclusions that instrumental effects were small and that hyperfine depolarization was complete thus providing an effective 'height' to the excited state charge density distribution. At 50 eV (figure 6 and table 7), the agreement is somewhat poorer but still quite satisfactory. At 80 eV (figure 7 and table 8) the very sharp decrease in the differential cross section with θ_e made data taking very time consuming at the larger θ_e. Thus data are only presented for $\theta_e \leqslant 20°$. It is seen that in this case also very reasonable agreement is achieved between measured P_4^M and data derived from Bartschat and Madison's (1987) results. If, as suggested earlier, the theory underestimates the negative-going excursion of P_1 around $\theta_e = 10°$ then even better agreement between experimental and theoretical P_4 data would be obtained.

The parameters, P_1 and ρ_{00}, which are appropriate to the nascent excited state charge cloud immediately following the original collision, have been evaluated for Kr and Xe as discussed in section 2 and are given in the tables. Figures 8 and 9 show the resultant ρ_{00} values for Kr and Xe along with theoretical predictions and the results of earlier workers. Within experimental error we find no deviation of ρ_{00} from zero in the range of θ_e considered. This is in complete agreement with both sets of theoretical

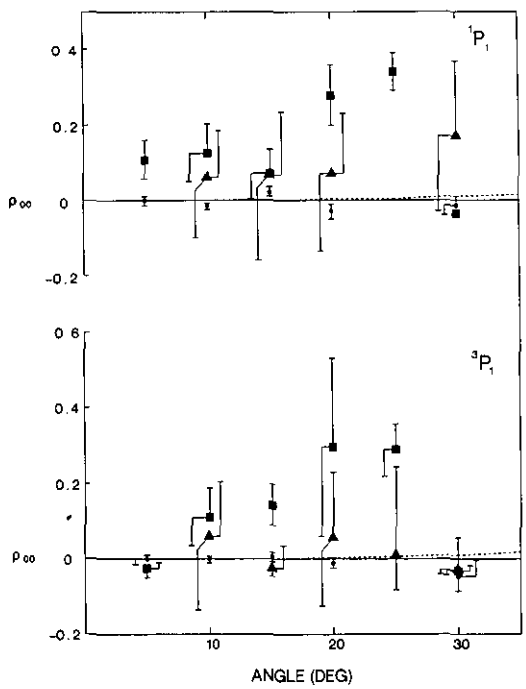

Figure 8. ρ_{00} parameter for electron impact excitation of the $[\frac{1}{2}]_1^0 5s'$ (top) and $[\frac{3}{2}]_1^0 5s$ (bottom) states of Kr at 60 eV incident energy. Circles, present data; squares, from Danjo *et al* (1985); triangles, from King *et al* (1985); full curve, Bartschat and Madison (1987) DWBA; broken curve, Meneses *et al* (1985) FOMBT. All the experimental data have been corrected to take account of hyperfine depolarization (see text).

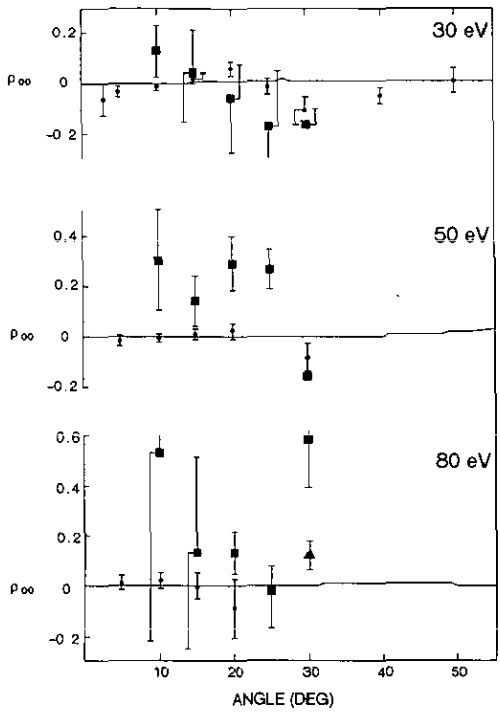

Figure 9. ρ_{00} parameter for electron impact excitation of the $[\frac{3}{2}]_1^0$ 6s state of Xe at 30 eV (top), 50 eV (middle) and 80 eV (bottom) incident energies. Circles, present data; squares, from Nishimura *et al* (1986); triangles, from McGregor *et al* (1982); full curve, Bartschat and Madison (1987) DWBA. All the experimental data have been corrected to take account of hyperfine depolarization (see text).

data and indicates that, in the angular range under investigation, no indication of any spin-flip in the excitation process is observed. We note that similar conclusions were reached by Simon *et al* (1990) in their careful study of small angle ($<10°$) scattering on Hg at 50 eV incident energy. They too highlighted the influence of hyperfine and interaction-region-geometry effects. We note also that this conclusion differs from that of Plessis *et al* (1988) who interpreted large deviations in their P_4^M values from unity in the cases of Kr and Xe as being evidence for spin-flip processes taking place. It is clear from the present work that this is not occurring.

It seems likely that the apparently non-zero ρ_{00} values reported earlier by Danjo *et al* (1985) and Nishimura *et al* (1986) (sse figures 8 and 9) using angular correlation techniques may also be explained using similar arguments to those presented in this paper. In figures 8 and 9 we have corrected the data from other laboratories to take account of hyperfine interaction effects. This allows a more meaningful comparison to be made with the earlier work.

5. Conclusions

Polarization correlation measurements of the P_1 and P_4 Stokes parameters have been presented for Ne, Ar, Kr, and Xe for incident electron energies in the range 30–80 eV

and electron scattering angles up to 50°. After adequate account was taken of finite-interaction-volume and nuclear spin depolarizing effects, good agreement was found with theoretical calculations. In particular, previous discrepancies between theory and experiment with regard to the charge cloud height parameter, ρ_{00}, have been resolved.

Acknowledgments

The financial assistance of the Natural Sciences and Engineering Research Council of Canada, Nato Division of Scientific Affairs (RG 686/84) and the Killam Foundation is gratefully recognized. The technical assistance of Mr Werner Grewe, Mr Bernard Masse and their staff is gratefully acknowledged.

References

Andersen N, Gallagher J W and Hertel I V 1986 *Proc. 14th Int. Conf. on the Physics of Electronic and Atomic Collisions (Palo Alto)* ed D C Lorents, W E Meyerhof and J R Peterson (Amsterdam: North-Holland) Invited papers pp 57-76

—— 1988 *Phys. Rep.* **165** 1-188

Bartschat K and Madison D H 1987 *J. Phys. B: At. Mol. Phys.* **20** 5839-63

Becker K, Dassen H W and McConkey J W 1984 *J. Phys. B: At. Mol. Phys.* 17 2535-48

Blum K 1981 *Density Matrix Theory and Applications* (New York: Plenum)

Blum K, da Paixao F J and Csanak G 1980 *J. Phys. B: At. Mol. Phys.* **13** L257-61

Blum K and Kleinpoppen H 1979 *Phys. Rep.* **52** 203-61

Danjo A, Koike T, Kani K, Sugahara H, Takahashi A and Nishimura H 1985 *J. Phys. B: At. Mol. Phys.* **18** L595-600

da Paixao F J, Padial N T and Csanak G 1984 *Phys. Rev.* A **30** 1697-713

da Paixao F J, Padial N T, Csanak G and Blum K 1980 *Phys. Rev. Lett.* **45** 1164-7

Hammond P, Karras W, McConkey A G and McConkey J W 1989 *Phys. Rev.* A **40** 1804-10

Hanne G F 1983 *Phys. Rep.* **95** 95-165

Hanne G F 1990 *Proc. 5th Int. Symp. on Polarization and Correlation on Electronic and Atomic Collisions (Hoboken)* (NIST Special Publication no 789) ed P A Neill, K N Becker and M A Kelley (Washington, DC: US Dept of Commerce) pp 128-33

Heath R L 1984 *Handbook of Chemistry and Physics, 64th Edition* ed R C Weast (Cleveland: The Chemical Rubber Co.)

Husson X, Grandin J-P and Kucal H 1979 *J. Phys. B: At. Mol. Phys.* **12** 3883-90

Jackson D A 1977 *J. Opt. Soc. Amer.* **67** 1638

Jackson D A and Coulombe M C 1972 *Proc. R. Soc. Lond.* A **327** 137-45

Johnson M C 1969 *Rev. Sci. Instrum.* **40** 311-5

Khakoo M A and McConkey J W 1986 *Phys. Rev. Lett.* **57** 679-82

—— 1987 *J. Phys. B: At. Mol. Phys.* **20** 5541-56

King S J, Neill P A and Crowe A 1985 *J. Phys. B: At. Mol. Phys.* **18** L589-94

Lederer C M and Shirley V S 1978 *Table of Isotopes 7th Edition* (New York: Wiley)

Machado L E, Leal E P and Csanak G 1982 *J. Phys. B: At. Mol. Phys.* **15** 1773-84

Martus K E, Becker K and Madison D H 1988 *Phys. Rev.* A **38** 4876-9

Martus K E and Becker K 1989 *J. Phys. B: At. Mol. Opt. Phys.* **22** L497-502

Matthias E, Rosenber R A, Poliakoff E D, White M G, Lee S T and Shirley D A 1977 *Chem. Phys. Letts.* **52** 239-44

McConkey J W 1979 *Symp. on Electron-Molecule Collisions* (Tokyo: University of Tokyo Press) Invited papers pp 163-78

McConkey J W, Hammond P and Khakoo M A 1988 *Electronic and Atomic Collisions* ed H B Gilbody, W R Newell, F H Read and A C H Smith (Amsterdam: Elsevier) pp 105-16

McConkey J W, van der Burgt P J M, Corr J J and Plessis P 1990 *Proc. 5th Int. Symp. on Polarization and Correlation in Electronic and Atomic Collisions (Hoboken)* (NIST Special Publication no 789) ed P A Neill, K N Becker and M A Kelley (Washington, DC: US Dept of Commerce) pp 115–20

McGregor I, Hils D, Hippler R, Malik N A, Williams J F, Zaidi A A and Kleinpoppen H 1982 *J. Phys. B: At. Mol. Phys.* **15** L411–4

Meneses G D, da Paixao F J and Padial N T 1985 *Phys. Rev.* A **32** 156–65

—— 1986 *Phys. Rev.* A **34** 675

Murray K D, Gough S F, Neill P A and Crowe A 1990 *J. Phys. B: At. Mol. Opt. Phys.* **23** 2137

Nienhuis G 1980 *Coherence and Correlation in Atomic Physics* ed H Kleinpoppen and J F Williams (New York: Plenum) pp 121–32

Nishimura H, Danjo A and Takahashi A 1986 *J. Phys. B: At. Mol. Phys.* **19** L167–72

Plessis P, Khakoo M A, Hammond P and McConkey J W 1988 *J. Phys. B: At. Mol. Phys.* **21** L483–8

Simon T, Sohn M, Hanne G F and Bartschat K 1990 *J. Phys. B: At. Mol. Opt. Phys.* **23** L259–63

Slevin J 1984 *Rep. Prog. Phys.* **47** 461–512

Slevin J and Chwirot S 1990 *J. Phys. B: At. Mol. Opt. Phys.* **23** 165–210

Wolcke A, Bartschat K, Blum K, Borgmann H, Hanne G F and Kessler J 1983 *J. Phys. B: At. Mol. Phys.* **16** 639–55

van der Burgt P J M, Corr J J and McConkey J W 1991 *J. Phys. B: At. Mol. Opt. Phys.* **24** 1049–67

Zetner P W, Trajmar S and Csanak G 1990 *Phys. Rev.* A **41** 5980–99

Zetner P W, Trajmar S, Casanak G and Clark R E H 1989 *Phys. Rev.* A **39** 6022